UNIVERSIDADE Ð COIMBRA

Hugo Tiago Teixeira da Ponte

AUTOMATIC RADIOTHERAPY TREATMENT PLANNING: ADAPTIVE APPROACHES

Julho de 2022

Agradecimentos

A conclusão desta dissertação de mestrado não seria possível sem o apoio de várias pessoas.

Em primeiro lugar gostaria de agradecer aos meus orientadores, a Professora Doutora Joana Matos Dias e o Professor Doutor Humberto Rocha. Obrigado pela oportunidade e pela esplêndida orientação que me deram, por estarem sempre prontos a ajudar, e a esclarecer tudo. O vosso apoio foi extremamente valioso.

Quero agradecer também a toda a minha família. Especialmente aos meus pais, pela ajuda, motivação e carinho dado ao longo dos últimos anos, sem vocês não teria sido possível a realização desta etapa. E aos meus tios Odete e Óscar, um obrigado por me terem recebido tão bem e por me fazerem sentir em casa quando eu estava longe dos meus pais.

Por fim, agradeço também aos meus amigos e colegas, em especial à Vera, à Eduarda, ao João e ao Carlos por estarem sempre por perto quando precisei de alguma coisa durante estes últimos cinco anos. Obrigado pelos bons momentos que me proporcionaram.

Um obrigado a todos.

Resumo

Objetivo: Em radioterapia, um plano de tratamento otimizado deve garantir uma cobertura adequada do volume a tratar (planning target volume – PTV) ao mesmo tempo que poupa todos os órgãos de risco (OAR). Como o tratamento é, geralmente, fracionado durante um determinado horizonte temporal, o replaneamento pode ser um passo importante na criação de um plano de tratamento otimizado, garantindo que a informação anatómica do paciente é atualizada e considerada durante o tratamento. No entanto, o replaneamento também tem desvantagens, devido à necessidade de adquirir novas imagens médicas e ao tempo adicional necessário para a criação de novos planos de tratamento. Este trabalho compara o uso de um planeamento robusto, tendo em conta estruturas auxiliares, com o replaneamento, tendo em conta o impacto na cobertura do PTV, poupando simultaneamente os OAR.

Métodos: Quatro abordagens diferentes de planeamento de tratamento são consideradas e comparadas. A abordagem convencional considera apenas a informação da tomografia computadorizada (CT) de planeamento, mantendo o mesmo plano de tratamento durante todo o tempo de tratamento. É testada uma nova abordagem robusta, onde são também tidas em conta 14 estruturas auxiliares que representam cenários possíveis para a evolução do PTV na criação do plano de tratamento inicial. Uma terceira abordagem considera fazer o replaneamento uma vez a meio do tempo total de tratamento. Uma quarta abordagem mimetiza o que é normalmente conhecido como o "plano do dia". Todos os planos de tratamento foram criados automaticamente recorrendo a um algoritmo baseado em sistemas de inferência difusos. Estas abordagens foram testadas num caso de cancro de cabeça e pescoço e foram comparadas usando simulação de Monte Carlo.

Resultados: Foi possível gerar automaticamente tratamentos clinicamente admissíveis para todas as quatro abordagens consideradas. O PTV obteve melhor cobertura com o planeamento robusto do tratamento.

Conclusões: Foi possível concluir que a abordagem robusta originou melhores planos de tratamento do que a abordagem convencional e que pode ser uma alternativa competitiva relativamente ao replaneamento durante o período temporal em que decorre o tratamento. A cobertura do PTV foi melhorada, garantindo as tolerâncias definidas para os OARs.

Abstract

Purpose: An optimized radiotherapy treatment plan must guarantee a proper coverage of the volume to treat (Planning Target Volume – PTV) while sparing all the organs at risk (OAR). As the treatment is usually fractionated during a given planning horizon, replanning can be an important step in creating an optimized treatment plan, by guaranteeing that the updated situation of the patient is being considered. However, replanning has also shortcomings, due to the need of acquiring new medical images, and additional time needed for creating new treatment plans. This work studies how the use of robust planning, taking into account auxiliary structures, compares with replanning, considering the impact on PTV coverage while maintaining proper OAR sparing.

Methods: Four different treatment planning approaches are considered and compared. The conventional approach considers only the information of the planning computed tomography (CT), keeping the same treatment plan during the whole treatment time. A new robust approach is tested, where fourteen auxiliary structures representing possible scenarios for the PTV evolution are also taken into account when creating the initial treatment plan. A third approach considers replanning once halfway of the treatment time. A fourth approach mimics what is usually known as the "plan of the day". All treatment plans were created automatically by resorting to an optimization approach based on fuzzy inference systems. These approaches were tested in a head-and-neck cancer case and were compared by Monte Carlo simulation.

Results: It was possible to automatically generate clinically admissible treatments for all the four approaches considered. PTV was better covered with the robust treatment planning.

Conclusions: It was possible to conclude that the robust approach originated better treatment plans than the conventional approach and it can be a competitive alternative to replanning. PTV coverage was improved, while properly sparing the OARs.

Key words: radiotherapy, treatment planning optimization, adaptive planning, medical physics

Acronyms

CT- Computed tomography

IMRT- Intensity Modulated Radiation Therapy

3DCRT- Three-Dimensional Conformal Radiation Therapy

GTV- Gross Target Volume

CTV- Clinical Target Volume

PTV- Planning Target Volume

OAR- Organ at Risk

MLC- Multi-leaf Collimator

VMAT- Volumetric Modulated Arc Therapy

TPS- Treatment Planning System

QA- Quality assurance

DVH- Dose Volume Histogram

BAO- Beam Angle Optimization

FMO- Fluence Map Optimization

DVC- Dose Volume Constraints

DAO- Direct Aperture Optimization

FIS- Fuzzy Inference System

MC- Monte Carlo

AAM- Average Anatomy Model

ART- Adaptive Radiation Therapy

D_{95}- Dose received by 95% of the volume

D_2- Dose received by 2% of the volume

D_{mean}- Mean dose

D_{max}- Maximum dose

V_{59}- Volume that receives 59 Gy

PTV70- Structure in study

Figure Index

Table Index

Contents

1. Introduction

According to the global cancer observatory, the number of new cases of cancer worldwide in 2020 was almost 19.3 million, 4.4 million of those being in Europe [1].

Prevention and an early diagnose are good measures to help dealing with cancer. According to the global cancer observatory, the 5-year survival rate in Sweden, Norway, Denmark, Finland and Iceland averaged 37.81% in 1970-1974 and 72.7% in 2015-2019 [2]. This was possible due to early diagnose, better prevention and due to novel/improved cancer treatments developed in the last few years. Many treatments can be provided according to the type and stage of the cancer, including radiotherapy, chemotherapy, surgery, stem cell transplant, immunotherapy, among others.

Radiation therapy (or radiotherapy) delivers high doses of radiation aiming to kill cancer cells by damaging their DNA. Cancer cells divide very fast but the cells that are damaged are unable to repair themselves as well as healthy cells. Since healthy cells can better repair themselves, the goal of the treatment is to deliver enough dose to compromise cancer cells but not enough to damage healthy cells beyond repair. This can be achieved by delivering radiation daily during several weeks. This fractionation aims at malignant cell destruction while preserving healthy tissue.

Radiotherapy can either use an external radiation source or use an internal radiation source (Brachytherapy). Brachytherapy is a method of internal radiation therapy in which seeds, ribbons, or capsules containing a radiation source are placed in the tumour region. There are several techniques for placing brachytherapy including: interstitial, intracavity and episcleral brachytherapy. Regarding the implant dose, implants can be qualified in three types: low-dose rate, high-dose rate, and permanent implants [3]. In external beam radiotherapy a machine is used to deliver radiation to the patient, treating a specific part of the body, using charged particles. The particle used to treat the intended area is chosen depending on the tumour and the type of interaction between the particle and the tissues.

External radiotherapy is delivered with the patient laying on a couch that can rotate. Radiation is generated by a linear accelerator, or linac, placed on a gantry that can rotate around a central axis parallel to the couch. When the couch is fixed at 0º the beam directions are called coplanar. Rotation of the gantry and the couch allows noncoplanar beams irradiating the tumour from almost any direction around the patient,

except for directions that would cause collisions between the gantry and the couch/patient [4]. Figure 1 depicts a linear accelerator.

Since the radiation is being delivered from different directions towards the tumour, it is possible to have a higher dose on the volumes to treat than on the surrounding healthy tissues. The main objective of radiotherapy treatment planning is thus to be able to calculate a treatment plan that irradiates adequately the volumes to treat while, at the same time, spares as most as possible all the surrounding organs, keeping their functionality.

Figure 1- Linear accelerator [5]

In this work, only external radiotherapy will be considered. The main focus of this work will be Intensity Modulated Radiation Therapy (IMRT), where it is possible to modulate the radiation delivered so that it better conforms with the volumes that should be treated.

As the treatment is usually fractionated, being delivered daily during a given number of weeks, the volumes to be treated, as well as the volumes that correspond to organs that should be spared, are not exactly the same during the whole treatment time. Changes in these volumes could be accommodated if new medical images were acquired and new treatment plans produced. However, this is not always possible, and acquiring new medical images during the treatment has also advantages and disadvantages, as discussed later on. The impact of changes in the volumes to treat and different approaches to take these changes into account are the main focus of the work developed. This work will be

focused on head-and-neck cancer cases, since one such case was used as a proof of concept for the approach developed, as described in section 7.

The main objective of the work to be developed is to understand the impact that changes in the patient throughout the treatment time period can bring to the quality of the treatment delivered, namely understand the importance of considering the replanning at some stage during the treatment. Four different approaches will be compared:

- Only one treatment is planned, and no other replanning is done during the course of treatment. This initial treatment plan is calculated considering only the existing structures of interest as defined in the planning computed tomography (CT).
- Only one treatment plan is considered during the course of treatment, but this plan is calculated considering not only the original structures of interest but also additional structures that are created and that represent possible changes to the Planning Target Volume (PTV) (it is, in some sense, a robust plan taking into consideration different potential scenarios for the PTV).
- Replanning is performed once during the course of treatment.
- Replanning is performed more often than the previous approach, mimicking the concept of the "plan of the day".

Computational results considering a head-and-neck cancer case are described.

This thesis is organized as follows. The next section gives a brief overview of the existing radiotherapy treatment modalities. In section 3 treatment planning and delivery workflow is introduced followed by a more detailed description of the radiotherapy treatment planning problems and how dose is calculated. On section 5 we explain what fuzzy inference systems are and how are they used to automate the treatment planning process. On section 6 the uncertainties related to the treatment are described as well as the adaptive planning role to mitigate some of these uncertainties. Finally on sections 7, 8 and 9 the computational experiments are described, and the main results and conclusions are discussed.

2. Radiotherapy Treatment Modalities

There are different radiotherapy treatment modalities. In clinical practice, standard treatment is done with photons. More recently, protons are also being used, taking advantage of their unique properties. Proton beams have unique depth-dose characteristics, since protons slow down as they penetrate matter, their rate of energy transfer increases with depth, coming to an abrupt stop just beyond where energy deposition is maximum producing the so-called Bragg peak. By positioning several Bragg peaks inside the target volume, excellent tumour irradiation is obtained, and adjacent organs at risk are spared [5].

In photon beam-based radiotherapy, it is not possible to avoid radiation being delivered beyond the target volume. In photon beam radiotherapy the most used therapies are 3D conformal radiotherapy (3DCRT) and intensity modulated radiation therapy (IMRT).

Regardless of the treatment modality, a CT scan of the patient is always needed to plan the radiotherapy treatment, where all the structures of interest are delineated by the medical doctor, namely PTVs and Organs at Risk (OARs).

In 3DCRT the target is irradiated by an array of beams individually shaped to conform with the 3D volume of the tumour, representing an increase in dose to the tumour and sparing of OARs when compared with its 2D counterpart, where x-ray images are used to delineate boundaries and a limited number of beams is used resulting in less conformity since the beams do not conform with the PTV. Although the shape of the beams conforms better with the volume to treat in 3D than in 2DCRT, the radiation intensity that is delivered is constant. There is no intensity modulation.

In 1982, IMRT was proposed by Brahme and, since then, this technique has been widely used all around the globe [6]. Initially, multi-leaf collimators (MLCs) were used in three-dimensional conformal radiation therapy (3DCRT) to define fixed field anatomical landmarks [7]. IMRT also uses a multi-leaf collimator to modulate the beams [8]. The MLC consists of pairs of leaves that can move side by side creating a variety of field openings (Figure 2). The leaf position must be accurate to less than a millimetre, since small deviations of the leaves can cause dose uncertainties of several percent [9]. The movement of the leaves originates the segmentation of each beam into a set of smaller imaginary beams with independent fluence (intensities), called beamlets, delivering a non-uniform radiation field to the patient [4], [10]. The main difference between 3DCRT and IMRT is that in IMRT it is possible to modulate the
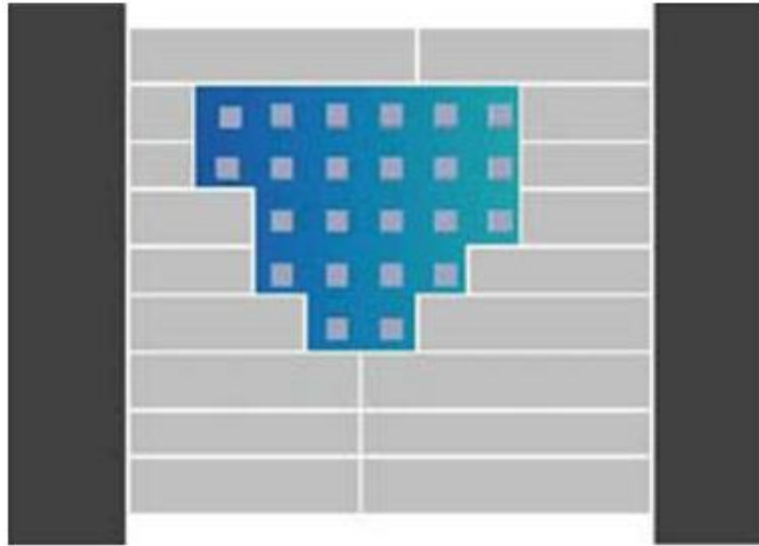
Figure 2- Illustration of a multi-leaf collimator [17]

fluence/intensity of the beam, which allows for a better tumour irradiation, and improved organ sparing [11]–[15]. IMRT treatment planning has an increased complexity when compared with 3DCRT treatment planning, since more decisions have to be made (increased degrees of freedom owing to the segmentation of the beams).

Volumetric modulated arc therapy (VMAT) is one of the most efficient radiotherapy methods, especially when accounting for dose delivery [16]. In VMAT, the gantry also rotates. However, instead of delivering the radiation from defined irradiation directions as step-and-shoot IMRT treatments do (radiation is only delivered from these defined directions, and radiation is off in all the position transitions), in VMAT the beam is always on, defining continuous irradiation arcs. The gantry speed, the dose delivery rate and the aperture of the MLC leaves are modulated [18].

Even though VMAT usually uses coplanar arcs (the couch is fixed), recent studies propose combining the short treatment times offered by VMAT [16], with the improved organ sparing from noncoplanar IMRT treatment plans [19].

CyberKnife is an example of a highly noncoplanar IMRT treatment modality. This modality also uses a linac with a highly manoeuvrable robotic arm, and integrated image guiding system, delivering both photons or x-rays. In this modality, the system based on the structures' contours creates a 3D representation of the tumour, defining the orientation of the beams based on this representation [20].

In the next section, only IMRT step-and-shoot treatments will be considered, since this is the focus of this work.

3. Treatment Planning and Delivery Workflow

The different treatment modalities share a common treatment workflow. A treatment plan requires a treatment CT scan (different from the diagnose CT scan) and a medical prescription. In the CT scan all the structures, OARs and PTVs must be well mapped (Figure 3). The OARs are the organs that may be exposed to radiation, while the PTV represents the volume of the known tumour including microscopic spread plus a margin around this volume. Other target structures commonly used include the gross target volume (GTV), that represents the volume of the known tumour and the clinical target volume (CTV) that adds microscopic spread to the GTV (Figure 4). Margins around target structures exist to compensate for eventual inaccuracies due to organ movement or changes in volume (bladder size, for instance) and patient movement.
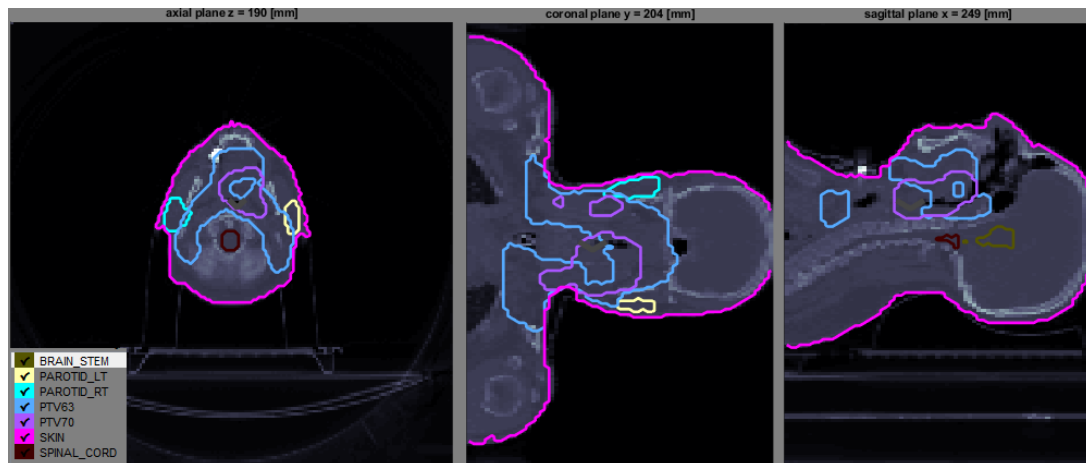
Figure 3- Delineated structures in a CT scan on 3 planes (axial, coronal and sagittal). In this image it is possible to see several delineated structures, namely two PTVs with different dose requirements, the spinal cord, parotids and brainstem.
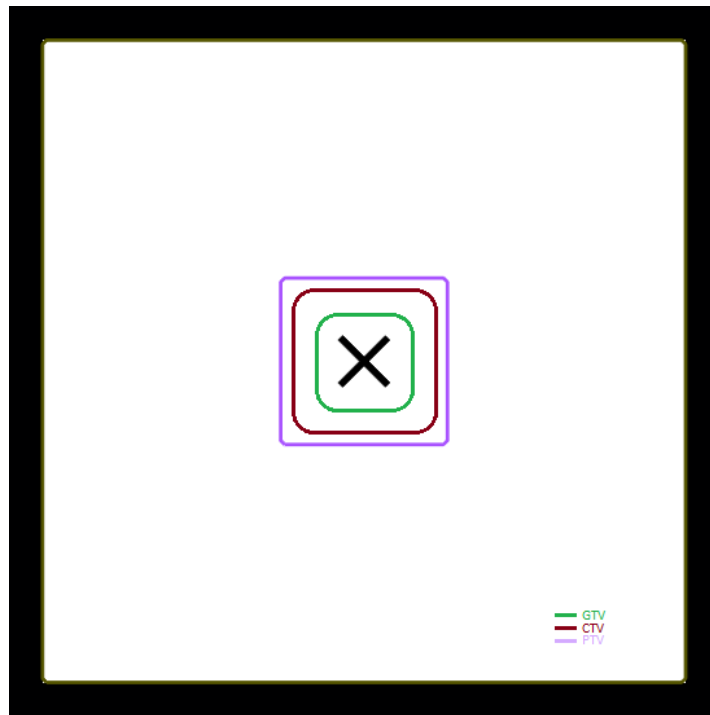
Figure 4- Schematic difference between GTV, CTV and PTV

All the structures of interest are discretized in voxels. Voxels are volumetric pixels where the length and width of each voxel depends on the resolution and spacing between the CT images [17].

Absorbed dose is the energy deposited per unit of mass of tissue and is expressed in Gray (Gy). The medical prescription, defined by the medical oncologist, is patient dependent and defines a set of dosimetric goals and constraints, for instance, maximum dose deposited in OARs and minimum dose deposited in PTVs. The definition of OAR constraints aims at preserving the organ functionality. Usually, two different sets of OARs are defined: serial and parallel organs. Serial organs are the ones that, if even only a small part of the OAR volume is damaged, the OAR functionality is jeopardized. In this case, usually the constraints define a maximum dose that cannot be surpassed at any voxel. Parallel organs are the ones that keep their functionality even if only a small part is damaged. In this case, the constraints usually define a mean dose threshold, taking into consideration the dose deposited in all the OAR's voxels.

Considering IMRT treatments, a treatment is planned when all the decisions have been made namely: the set of radiation directions that is going to be used (including the position of the couch for non-coplanar treatments), the radiation intensities (also known as fluence map) associated with each of those directions and the position and movement of the multi-leaf collimator leaves that will originate the desired fluence maps.

Given the complexity of IMRT treatment planning, the planner is assisted by a dedicated software, called Treatment Planning System (TPS). In this TPS, the planner is asked to define several parameters associated with the structures of interest, like lower and upper dosimetric bounds or weights. Then, the TPS optimizes a given mathematical model that tries to define the treatment plan taking into consideration these defined parameters. This mathematical model has a given objective function that is usually minimized and shaped by the parameters chosen by the planner. This procedure is usually known as inverse planning. After the initial treatment plan is defined, the doses absorbed by all the structures of interest are calculated. If the dose distribution meets the medical prescription the procedure finishes, unless the planner thinks it is still possible to improve either OAR sparing or PTV irradiation beyond what was defined in the medical prescription. If the calculated doses do not comply with the prescription, or the planner is aiming at further improvements, one or more parameters are updated, and a new treatment plan is calculated. In this lengthy trial-and-error procedure, the planners typically resort to their own experience, and the resulting plans may not even be the best ones in terms of sparing critical organs or the achievement of proper PTV irradiation [21].

Quality assurance (QA) must be done throughout the entire treatment, from the diagnose CT to the delivery of the treatment. Since the focus of this work is the treatment plan, only the QA of the plan will be discussed.

There are many ways by which a given treatment plan is assessed. Measures like conformity, homogeneity and coverage are calculated. Conformity is defined as the ratio between the PTV and the irradiated volume; homogeneity is defined as the uniformity of the dose distribution of the PTV; coverage is the ratio of the PTV covered by the isodose surface prescribed to the total PTV [17]. To ensure the quality of the treatment plan, dose volume histograms (DVH) are also commonly used. DVH shows the amount of radiation that a certain structure receives as a function of the volume, allowing to analyse and compare different plans and dose distribution on each structure (Figure 5). Isodose graphic representation is another tool that is used to evaluate the quality of the treatment [17][22]. Hotspots (ratio between the maximum dose received by any of the voxels in a structure and the prescribed dose above a given threshold) and coldspots (ratio between the minimum dose received by any of the voxels in a structure and the prescribed dose under a given threshold) must be prevented. Hotspots can cause permanent damage to OARs and coldspots will allow the tumour to grow and spread [23].
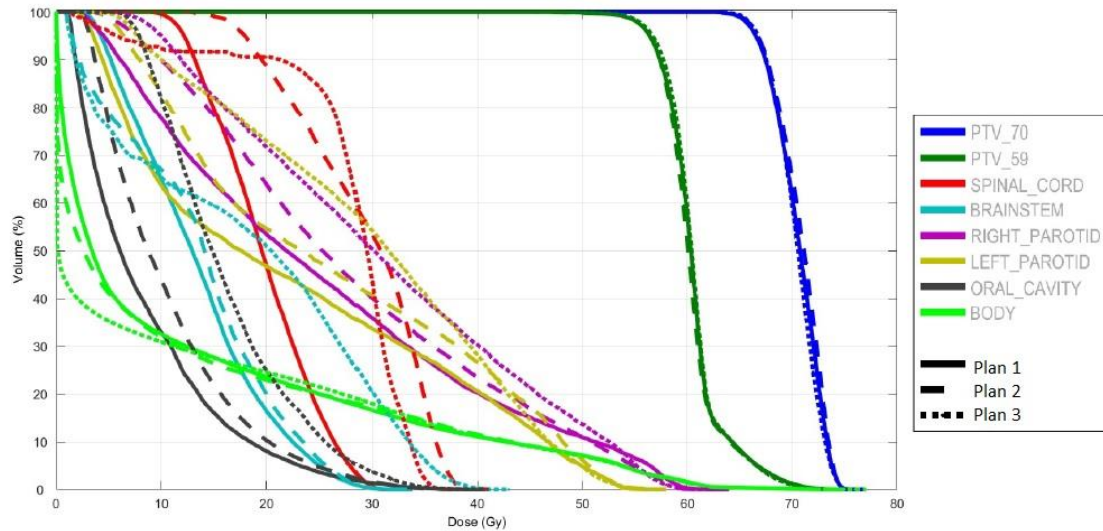
Figure 5- *Illustration of a DVH comparing different head-and-neck treatment plans*

4. Radiotherapy Treatment Planning

Treatment planning is typically organized in 3 different stages. These stages are now detailed.

4.1 Beam angle optimization problem

In IMRT, the beam angle optimization problem (BAO, also known as the geometry problem) considers the decisions that have to do with the position of the patient and of the irradiation beams. BAO is very important since it helps to achieve or improve organ sparing, PTV coverage and it directly influences the treatment time. Treatment time is important for two different reasons: if treatments take shorter times, more patients can be treated, and this can be important in terms of the number of patients that a given institution can treat. For each patient, shorter treatment times are not only more comfortable, but they also decrease the probability of the patient moving, causing the PTV and OARs to change their position [17].

The geometry problem is divided in two parts: deciding how many irradiation beams to use; deciding which angles to use. In clinical practice, the number of beams to use is usually defined *a priori*, considering the location of the PTVs, specific characteristics of the patient and the experience of the planner and of the institution. The directions (angles) are usually chosen by the treatment planner, using a trial-and-error

approach that is time consuming, and in most cases are not optimized, since TPS do not yet offer good beam angle optimization tools.

Breedveld *et al.* shows that, for different cases, noncoplanar angles using BAO outperformed coplanar beam angles [24].

Rocha *et al.*, tackles this problem offering an alternative continuous approach considering noncoplanar beams, obtaining improved results when compared to the coplanar equidistant beam angles [25].

4.2   Intensity/Fluence map optimization problem

The fluence map optimization (FMO) problem consists of finding the optimal beamlet intensities (weights) for the previously chosen beam angles. There are many mathematical optimization models that address this problem, including linear models, non-linear models, mixed integer linear models and multiobjective models. In the medical prescription, goal dose for tumours, maximum and/or mean dose values for OARs and the rest of the body are established. With the evolution of IMRT inverse planning systems it is possible to define dose-volume constraints (DVC) stating that only a certain fraction of a structure can be exposed to a dose value higher (lower) than the upper (lower) threshold. With the definition of DVCs it can be easier to better represent the goal of improving tumour dose without damaging nearby OARs [26].

The dose for each voxel is calculated using the superposition principle, where we consider the contribution of each beamlet. A dose matrix, D, is obtained from the unitary fluence of each beamlet. It has information on the absorbed dose in each voxel, from each beamlet, considering radiation intensity equal to 1. In this matrix, each row corresponds to one voxel, and each column corresponds to one beamlet. The dose received by voxel i, d_i, can be represented as the sum of the contribution of each beamlet, $d_i = \sum_{j=1}^{N_b} D_{ij}\, \omega_j$, where N_b is the total number of beamlets, ω_j is the intensity of the beamlet j and D_{ij} represents the elements in the ith row and j^{th} column of matrix D (absorbed dose in voxel i from beamlet j, considering beamlet j has unitary radiation intensity). The matrix D is a very large matrix, since the total number of voxels, N_v, can reach tens of thousands, which makes the fluence optimization harder. To minimize the size of the matrix, the number of voxels can be decreased, and one of the strategies used is known as sampling, where a given number of voxels of certain structures will be assembled into one voxel.

Most models use one objective function that is intended to be minimized. We give as an example a model that will be used as the starting point of this work, and that considers the minimization of a quadratic objective function with no additional constraints. For each and every voxel, the dose received is compared with a given threshold. The function will be

penalized if there is a difference between the received dose and the desired/allowed dose for that voxel. These differences are squared in order to obtain a convex problem that is easier and faster to solve. With this model, it is possible to allow small dose differences without big penalizations but if the deviation is too large it will be greatly penalized. This model is represented in Equation 1.

$$min_{\omega \geq 0} \sum_{i=1}^{N_v} \left[\underline{\lambda_i} \left(T_i - \sum_{j=1}^{N_b} D_{ij}\, \omega_j \right)^2_+ + \overline{\lambda_i} \left(\sum_{j=1}^{N_b} D_{ij}\, \omega_j - T_i \right)^2_+ \right] \qquad (1)$$

where T_i is the desired/allowed dose for voxel i, $\underline{\lambda_i}$ and $\overline{\lambda_i}$ are the penalties of underdose and overdose of the voxel i, and $(.)_+ = max\{0, .\}$ [21]. Although the values for the parameters used in this model can be related with the dose volume constraints defined by the medical prescription, they can be changed and they can be quite different from these goal values, as this objective function value has no clinical meaning. The objective of any optimization mathematical model that is used in inverse optimization is to be able to lead to solutions (optimal solutions of the mathematical optimization model used) corresponding to treatment plans that comply with the medical prescription. Hence, the models used must be able to drive the search for this treatment plan towards interesting regions of the searchable solution space.

4.3   Realization Problem

After the intensities are optimized, we have a fluence map that is continuous (Figure 6). The next step considers the optimization of the movement of the leaves so that the calculated fluence map is delivered. This problem is usually known as the realization problem.
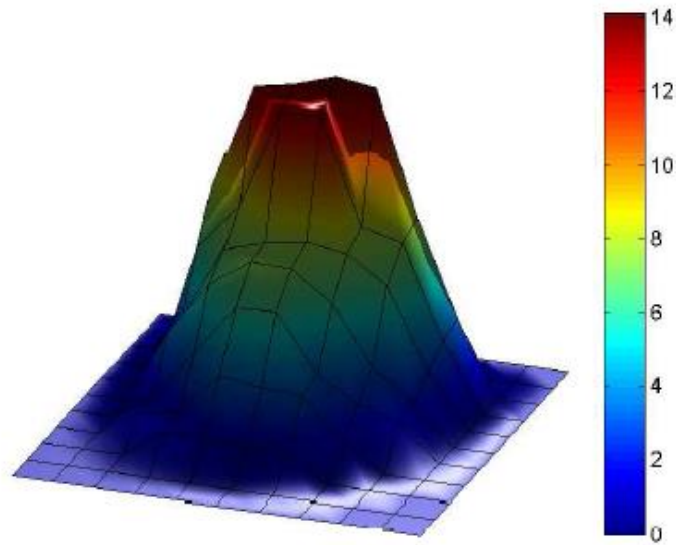
Figure 6- Fluence map obtained in the end of the optimization process [27]

The movement of the leaves does not allow the delivery of the continuous fluence map calculated. Since the beams are discretized into beamlets, the delivered fluences are not exactly the same as the ones that were calculated in the fluence map optimization due to the MLC device restrictions. So, there is always some loss associated with this discretization, as can be seen by the differences between Figures 6 and 7 that try to depict this situation. Figure 6 displays the optimal fluence calculated. This fluence is then discretized (Figure 7) and delivered by the movement of the leaves (Figure 8).

The realization problem has been tackled by many authors using different techniques, aiming to obtain deliverable fluence maps as close as possible to the optimal ones, minimizing the loss incurred due to this discretization [28]–[31].

Regarding the movement of the MLC leaves, two different situations can be considered: dynamic collimation, where the radiation is on while the leaves move, and multiple static collimation or "step-and-shoot" mode, where the leaves will open a desired aperture during each segment of delivery and radiation is interrupted when the leaves move [17].

Instead of considering the fluence map and realization problem as separate and sequential problems, there is also the option of tackling these two problems at once. Direct aperture optimization (DAO) is a method first introduced by Shepard *et al.* [28], whereby using an automated planning system, the shape and weights of the apertures are optimized. DAO approaches have, as main advantage, the explicit inclusion of the discretization that inevitably exists by the movement of the leaves. However, these approaches lead to optimization problems of higher dimensions, increased degrees of freedom, and that can be harder to solve.
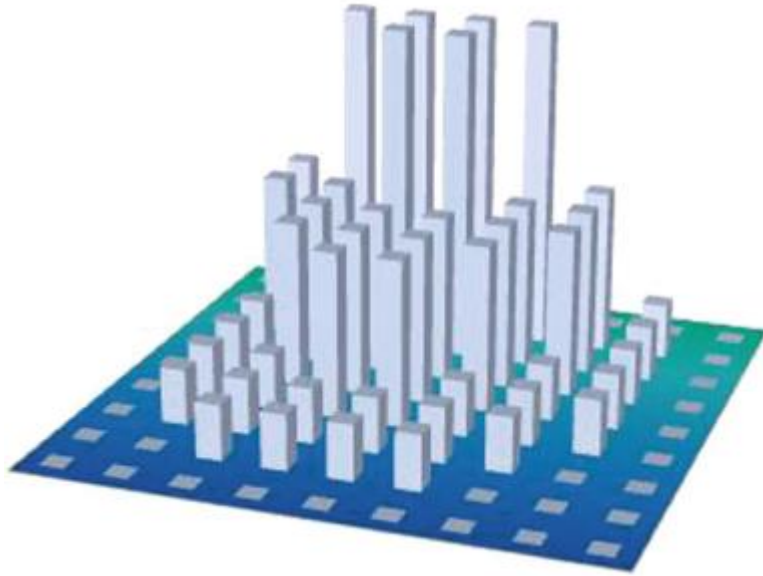
Figure 7 *- Discrete intensity map obtained by discretizing the continuous fluence map of Figure 6* [17]
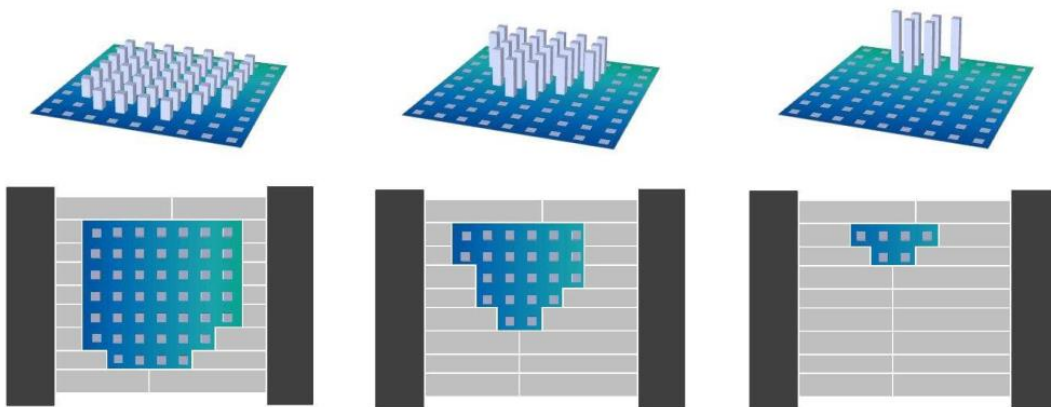
Figure 8 *- Decomposition of the fluence map in Figure 7. Through the superposition of the apertures the fluence map of Figure 7 is obtained* [17]

4.4   Treatment Planning Automation

As already described, treatment planning is still heavily relying on a time-consuming trial-and-error process, with a result that is highly dependent on the planner's experience and time availability. A planner may need hours or even days to reach a high-quality treatment plan, that fulfils the medical prescription. Therefore, many efforts have been put in trying to make treatment planning partially or fully automated. The automation of treatment planning is not a new idea and, looking at the existing literature, it is possible to find many works addressing this concern. Important advancements were achieved, mainly relying on optimization

approaches for beam angle optimization in IMRT, arc trajectory definition for VMAT and FMO. Zhang *et al.*, propose a treatment plan approach for lung cancer where the beam angles were selected through a treatment plan expert database [32]. Optimization parameters associated with OARs can be adjusted throughout the process depending on the objective function values of the current solution. Zarepisheh *et al.*, propose a treatment planning optimization based on the DVH curves of a reference plan, where voxel weights used in the FMO objective function are automatically updated by projecting the current dose distribution on the Pareto surface of the problem, considering the corresponding gradient information (the Pareto surface is defined by all the compromise solutions, meaning that it is not possible to improve one goal without worsening another one) [33]. Jia *et al.*, propose a treatment plan procedure in an OAR 3D dose distribution prediction [34]. Instead of having a medical prescription guiding the FMO, these predictions are the dosimetric references for OAR objectives. The FMO objective function is not dynamically updated taken into consideration the current solution dosimetric achievements. No beam angle optimization was considered [34]. Schipaanboord et al. , propose a fully automated treatment planning procedure for robotic radiotherapy [35] and Bijman *et al.*, for MRI-Linac (uses magnetic resonance imaging to monitor the target area at the same time the treatment is being delivered) applied to rectal cancer [35], [36]. The plan generation is based on a previous approach named Erasmus iCycle [24]. This method requires that a fixed wish-list is previously defined to be used for all the patients with the same tumour location. The need to fix *a priori* all the parameters in the wish-list can be a disadvantage for some patients that have specific situations that deviate from the most common cases. The selection of beam angles was based on an iterative selection process, where one beam is fixed at each iteration. Wortel *et al.*, suggest an automated plan via protocol based automatic iterative optimization. The authors define a set of treatment templates that achieve good results when used with the Pinnacle3 16.2 Auto-Planning TPS [37]. Cilla *et al.*, compare the new personalized algorithm implemented in Pinnacle3 for full planning automation of VMAT prostate cancer treatments with the previous mentioned auto-planning tool. Both the procedures are based on an *a priori* defined templates [38].

A new fully automated FMO procedure, where all the objective function parameters (weights and bounds) are tuned based on fuzzy inference systems (FIS) was presented in Dias *et al.* [39]. With FIS it is possible to mimic the human planner reasoning, considering a simple optimization model as defined in equation (1). The bounds in equation 1 are initially defined according to the medical prescription, while the weights' values are considered equal to 1 except in certain situations (e.g., overlapped PTVs). The fuzzy inference mechanism is composed of different sets and rules that will iteratively decide how much the bounds and weights must

be changed, using common sense rules (if a restriction is violated, the bounds and weights are changed until satisfied) [39]. Since this is the method that we are going to use for automatic FMO, section 5 describes this approach in more detail.

4.5   Dose Calculation

The treatment planning procedure requires dose to be calculated for each patient's voxel at each iteration when inverse optimization is performed. There are different ways of calculating the deposited dose. Some are more accurate but computationally more demanding (based on Monte Carlo simulation), others are faster but not as accurate (pencil beam algorithms).

Both pencil beam and Monte Carlo (MC) algorithms are kernel-based algorithms. These algorithms use a kernel to model dose deposition at a given point, where a kernel is a model of the energy spread at a given point.

The pencil beam dose calculation technique has as its basis the fact that the photon beam hitting the patient is composed of several smaller beams, the so-called pencil beams. Pencil kernel is then applied to each of the smaller beams giving each a specific dose distribution, which are then summed together obtaining the dose map. While pencil beam has similar results as Monte Carlo in homogeneous tissues [40], it has limitations with anatomical regions where heterogeneities exist [41]. However, pencil beam requires less computation time than Monte Carlo and, therefore, it is much faster.

MC allows computing dose distributions by simulating interactions of a large number of rays where the energy released is detected through the use of probabilities [40]. Since MC simulates a large number of interactions it is computationally demanding, but the results have increased precision.

In clinical practice, most of the times pencil beam dose calculation is used in the trial-and-error procedure, but for the final treatment plan the dose is calculated using Monte Carlo based algorithms, for increased accuracy and better quality control.

5. Automated FMO by Fuzzy Inference Systems

Since its proposal, fuzzy sets have been used in multiple fields from engineering to medicine, due to its various capabilities such as fuzzy optimization, image processing, among others.

Dias et al. [37] propose the use of fuzzy inference systems (FIS) to mimic the planner's procedure in an automated, efficient, and optimized way due to its flexible structure. Fuzzy inference systems allow for the automation of the FMO treatment planning, by iteratively changing both weights and bounds in (1) based on a reasoning similar to the human planners.

The algorithm will, in an iterative way, change upper and lower bounds trying to achieve PTV coverage while respecting the constraints that guarantee proper OAR sparing. If this is not enough, structure weights will also be changed in an iterative way. According to Dias et al., changing weights first makes it harder to control the behaviour of the optimization model [39].

In this methodology, the planner can attribute priorities to both OARs and PTVs within a certain range, but this is not mandatory. PTV priorities will be used to help improving treatment constraints, trying to irradiate the PTVs even more than it was defined in these constraints, while OARs with higher priority will be further spared.

Bounds and weights are changed based on common-sense rules, where if a given dose constraint is being violated, the respective bound or weights will be changed so that the constraint is satisfied.

Lower and upper bounds are initialized based on the medical prescription. Upper and lower bounds are assigned to PTVs while OARs only need upper bounds. OARs only have dose volume constraints that consider upper bounds, whilst PTVs have usually dose volume constraints that consider both upper and lower bounds (it is necessary to guarantee, for instance, that 95% of the volume receives at least 95% of the prescribed dose but, at the same time, to guarantee that no voxel receives more than 107% of the prescribed dose).

In the beginning, all structures can have the same weight equal to 1, meaning that every voxel has the same weight regarding the optimization process. A different situation occurs when two or more PTVs with different defined dosimetric constraints are overlapping, which happens often. In this case, the voxels that belong to the smaller volumes are associated with higher weights than the others. If some OARs are harder to spare, for instance, they can be associated with higher weight values right from the start. These initial values are not very important, as they will be changed

automatically by the algorithm, but can have an impact on the total computational time needed to reach an admissible plan.

Fuzzy numbers allow for the mathematical representation of concepts, that humans easily understand in natural language, but that are difficult to assign to crisp numbers. Fuzzy sets do not have clearly defined boundaries, allowing for a certain input to belong to more than one set with a given degree of membership.

The planners' reasoning can be expressed by a set of simple rules in natural language: if, for a certain structure, the deviation between the received dose and the prescribed dose is low/medium/large, then the respective upper/lower bound should be slightly/medium/greatly increased/decreased. The further away the structure of interest is from what is desired, the more pronounced the change of the respective parameter should be. Fuzzy numbers allow for the mathematical representation of these concepts, like *low*, *medium* or *large*. For example, a given deviation can belong to both *low* and *medium* sets with different degrees of membership, that do not need to add up to 1. The membership functions allow to define what *low*, *medium* and *large* deviations are (see Figure 9 for an example). The percentage of deviation between the prescribed/accepted dose and the received dose is the input, while the percentage of change in a particular bound is the output. Inputs and outputs are connected through fuzzy rules. All rules of the FIS are evaluated simultaneously, even if some of them are not in use (are not activated). Through a procedure usually known as defuzzification, a final and crisp value is obtained from the truncated output fuzzy sets, Figure 10 [39].
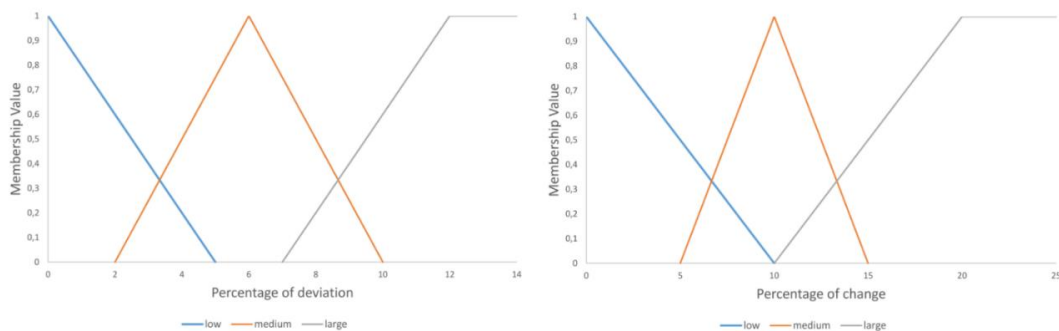
Figure 9- Input and Output membership functions [39]
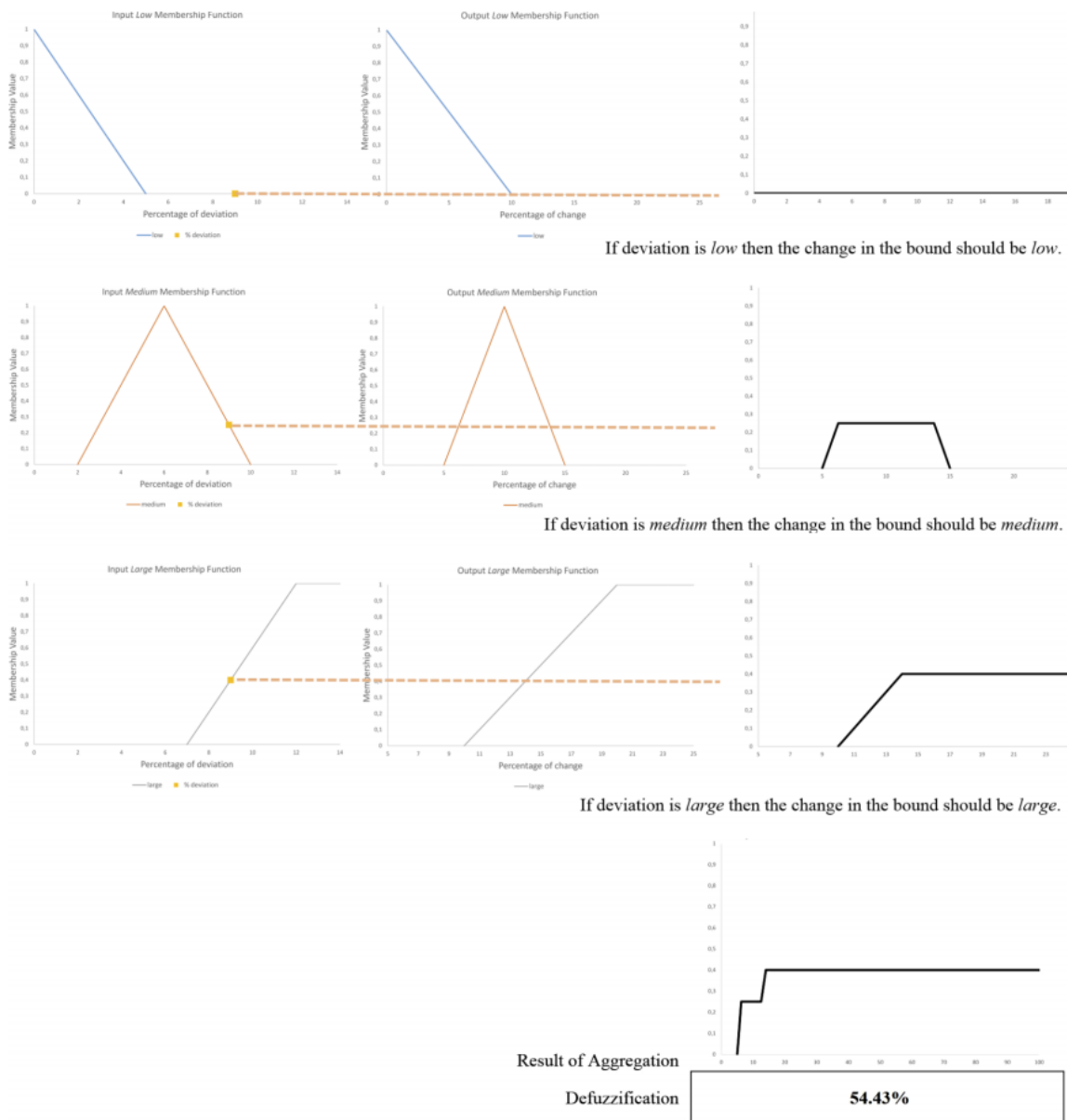
Figure 10- How to obtain a value from the fuzzy function using defuzzification [39]

Weights are changed in a similar way as bounds. The fuzzy rules and input functions are similar, while the output function is slightly different. It is important to limit the change that the algorithm can do to the weights in order to enable reaching an admissible solution. Each time the weights are changed the bounds are reset and return to their initial values, repeating the process until a solution is found. Figure 11 depicts the FIS flowchart.

In the original version of this approach, after an admissible solution is found, the algorithm will be increasingly more demanding, further improving PTV coverage. Finally, the algorithm will try to spare OARs beyond the tolerances defined. Further improvements to OAR sparing are made while maintaining the achieved PTV coverage.
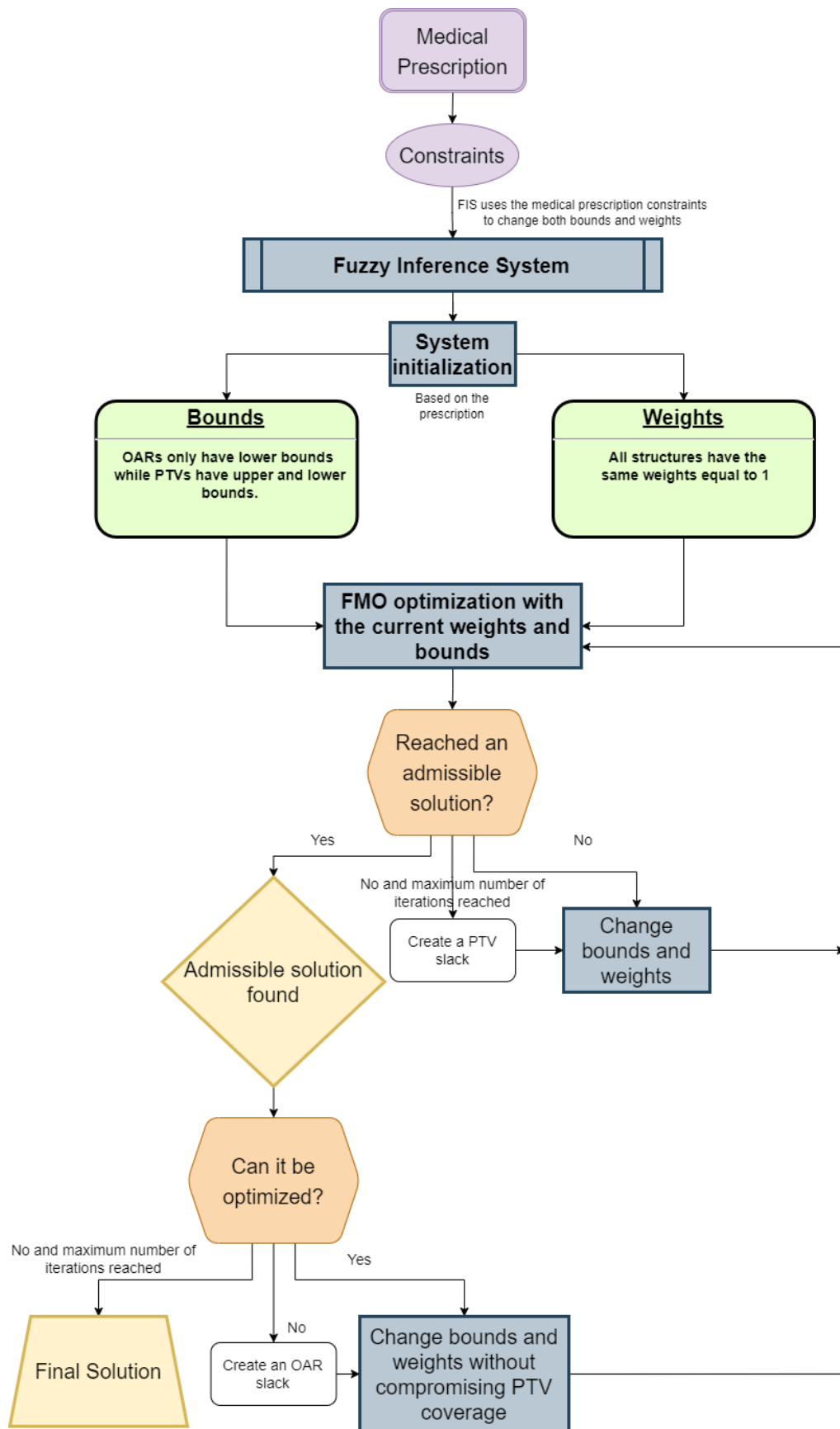
Figure 11- FIS Flowchart

6. Uncertainties and Adaptive Treatment Planning

The planning CT represents the patient on the day the medical image was acquired. However, there is a time lag between this CT being acquired and the treatment being initiated. Furthermore, as the treatment is divided into a set of daily fractions, the patient's anatomy changes as the treatment progresses, possibly leading to discrepancies between planned and delivered dose distributions. These discrepancies can lead to a decrease in the probability of tumour control, or increased probability of OAR complications.

According to Sonke et al. there are three types of anatomical changes that can induce errors [40]:

- During the acquisition of the planning CT, the patient is placed in a given position that will be replicated during the course of the treatment. Although the patient positioning is as accurate as possible, and different techniques are used to guarantee this proper positioning, it is not possible to eliminate completely this error, and there is usually a systematic positional error [42].
- The treatment delivery is composed of multiple sessions and the patient positioning should remain the same along all the sessions. This is not an easy task, since the sessions are done in different times, with different personnel, changing the reproducibility conditions [43]. Several techniques are used to immobilize the patient during the treatment based on the location of the PTV [44]. There are also anatomical changes of the patient that can occur between different treatment fractions and that are usually considered as being random errors.
- The treatment can also cause gradually increasing changes in the structures of interest that contribute to both systematic and random errors, due to the treatment effect over both PTVs and OARs (the PTV may decrease, the patient can lose weight, for instance).

Patient's CT is one of the most important data for structure delineation and dose calculation. This CT will give important information about organ density and structure location. There can be uncertainties considering tissue density information that is retrieved from the CT, and that can contribute to dose calculation uncertainties, along with random errors due to detector response, detector positioning and systematic errors due to the detector response [43]. During the treatment delivery, uncertainties like patient movement (voluntary and involuntary movements such as respiratory movements), structure movement (relative to what was

defined in the CT scan), structure size (bladder size changes, for instance) and patient positioning can also be present.

The fractionation of the treatment, and the impact of the dose that is delivered, can make the initial planning CT obsolete, in the sense that it is no longer representing the current situation of the patient. Patients that are doing concomitant chemotherapy treatments, for instance, can lose weight. If these changes are pronounced, a replanning is needed: a new CT must be acquired, and a treatment replanning takes place.

Adaptive radiotherapy (ART) was introduced as a method to reduce the effects of patient related uncertainties during the course of the treatment, achieving better results during the treatment. Adaptative plans can bring important advances in treatment quality since the patient and tumour evolution are considered during the treatment [45].

The PTV and the surrounding organs can change their disposition and/or size during treatment, therefore it is important to account for and manage these changes. Several authors have studied anatomical modifications during radiotherapy. Barker *et al.* show that, for head and neck cancer cases, the GTV decreased 69.5% with asymmetrical shrinkage and with a centre of mass displacement of 3.3 mm, while the parotid glands decreased $0.19 \, cm^3$ per day of treatment with a median displacement of 3.1 mm. The authors conclude that these changes can have a potential dosimetric impact and suggests that adaptive planning can be made based on the treatment-related anatomical changes [46]. Hansel et al. work describe a right and left parotid glands size decrease of 15.6% and 21.5%, respectively, but no GTV reduction [47]. Osorio *et al.*, show that both the GTV and parotid glands decreased in volume [48]. The GTV decreased 25±15% while the parotid glands in the same side of the tumour and in the opposite side saw a 17±7% and 5±4% decrease, respectively.

The average anatomy model (AAM) allows the treatment to be changed based on the previous fraction of the treatment. The AAM can be estimated based on the planning CT and first few CTs, calculating the average deformation vector field or changing the initial planning scan and corresponding structures accordingly. The replanning is performed when anatomical changes of the patient exceed a certain threshold [49]. Scheduled adaptation allows for a specific replan occurrence, either once or several times during the treatment. Scheduled adaptation removes the existing disadvantage of triggered adaptation since the patient anatomical changes are unpredictable, therefore not always able to trigger the adaptation process [50].

The increase of the number of times a replanning is performed converges to the concept of the "plan of the day". In this case, based on a daily CT, the treatment can be replanned also daily and immediately before the

treatment is delivered. The technique allows for better PTV coverage and organ sparing [51]. However, daily replanning comes at a cost, and some disadvantages can also be identified. One of the issues is the total radiation delivered to the patient due to the increased number of CTs that are acquired. This radiation is not, most of the times, accounted for when calculating dosage delivery to each structure. Furthermore, whenever a CT is acquired, all the volumes of interest must be delineated (which is not yet a totally automated procedure), and a new plan must be calculated, which takes time. This can have an important impact in the treatment delivery workflow, and also on the total number of patients that can be treated daily. In this work we are not considering the use of MRI-Linac, where it is possible to integrate magnetic resonance imaging machine with a linear accelerator.

7. Materials and Methods

7.1   Head and neck cancer case

To compare the different treatment planning approaches, a head-and-neck cancer case was used. This case is available in matRad, the open-source treatment planning system for academic research that we have used in this work.

Treatment planning for head-and-neck cancer cases is usually a very complex procedure, since there are many organs very close to, or even overlapping, the volumes to treat.

In the case considered, four OARs were included in the treatment plan optimization (right and left parotids, brainstem, spinal cord), in addition to two PTVs with different medical prescriptions that are partially overlapping (Figure 12). All the voxels that do not belong to any of these structures of interest are assigned to an OAR usually named as Body or Skin. This OAR is also important in treatment planning because it has to be guaranteed that no hotspots appear in the patient outside the structures of interest delineated. OARs like the spinal cord and brainstem are serial organs meaning that if some part of these organs is damaged, the organ's functionality will be compromised. Therefore, a maximum dose is established for these organs. The parotids are parallel organs, meaning that if a small part of the structure is damaged, the organ may keep functioning. The tolerance defined for these organs depends on the size of the volume irradiated, therefore mean dose is usually the objective type considered for these organs.
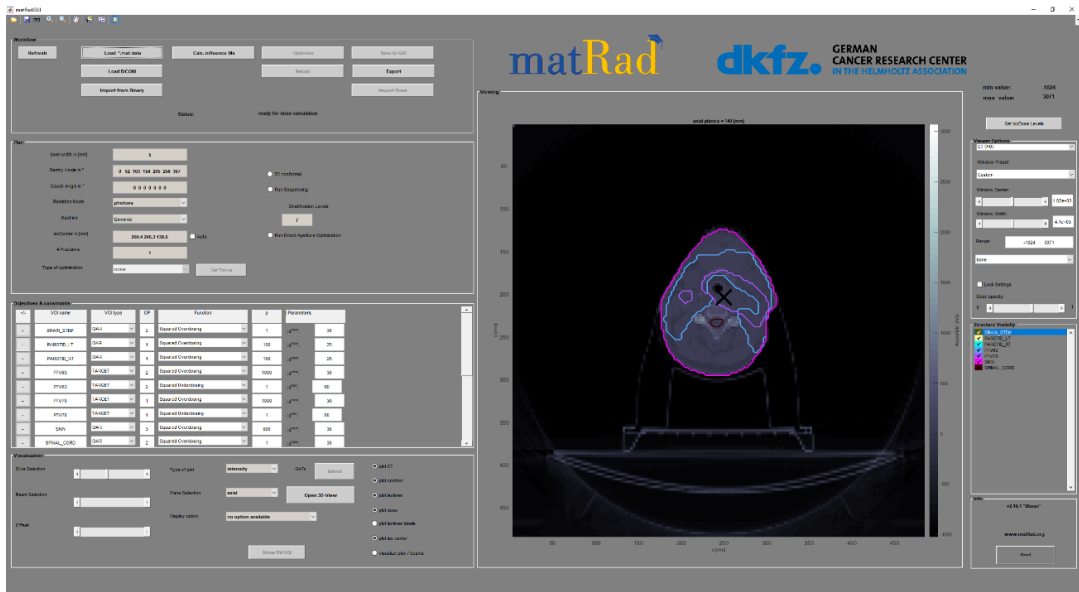
Figure 12- *Head-and-neck cancer case from matRad [48]*

For the PTVs, the usual medical prescription determines that a given percentage of the volume has to receive at least a given dose. In this case, the dose of 95% of the volume (D_{95}) is considered, and this value has to be at least 95% of the prescribed dose. If the prescription dose is equal to 70Gy, for instance, then, D_{95} should be greater than or equal to 66.5Gy, meaning that at least 95% of the PTV volume has to receive at least 66.5 Gy. In this case, one PTV has a medical prescription of 70Gy (named *PTV70*), the other one of 63 Gy (named *PTV63*).

The medical prescription for each of the 7 original structures are described in Table 1.

Table 1- *Medical prescription for a head-and-neck cancer patient in Gray (Gy)*

Structure	Type of constraint		Limit
Brain Stem	Maximum dose	Lower than	54
Left Parotid	Mean dose	Lower than	26
Right Parotid	Mean dose	Lower than	26
Skin	Maximum dose	Lower than	80
Spinal Cord	Maximum dose	Lower than	45
PTV63	D_{95}	Greater than	59.85
PTV70	D_{95}	Greater than	66.5
PTV70	Maximum dose	Lower than	74.9

7.2 Treatment planning strategies

BAO might play an important role in the final treatment plan quality. However, it is a very challenging problem that is seldom addressed in clinical practice. Instead, coplanar equispaced beam configurations are common in practice. Therefore, we used seven fixed, equidistant coplanar angles without optimizing the chosen set.

Although all the structures of interest are expected to change during treatment, in this work a simplification has been assumed and only PTV70 was considered as being changed during treatment, keeping unaltered all the other structures. We decided to only consider the case where the target volume decreases in size, which is the majority of cases [46], [48]. No other uncertainties are considered, like systematic or random positioning errors.

The tumour volume (PTV70) was randomly and iteratively changed to simulate asymmetrical size decreases during the treatment course. These changes were calculated as follows: based on the current PTV70, considering small and randomly generated displacements in the x, y and z axes relative to its current position, auxiliary structures were created. The intersection between the current PTV70 and one of the new auxiliary structures gives rise to a new PTV70 that corresponds to an asymmetric reduction of the original structure. Figure 13 illustrates this procedure.
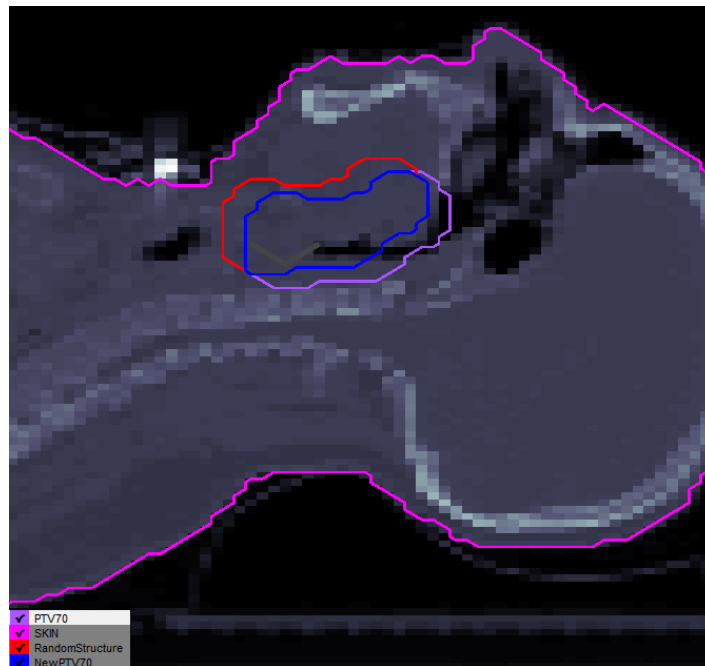

Figure 13- Generating an auxiliary structure by randomly shifting the PTV70. The intersection of the voxels of the original PTV70 and this auxiliary structure results in a new randomly generated reduced PTV70
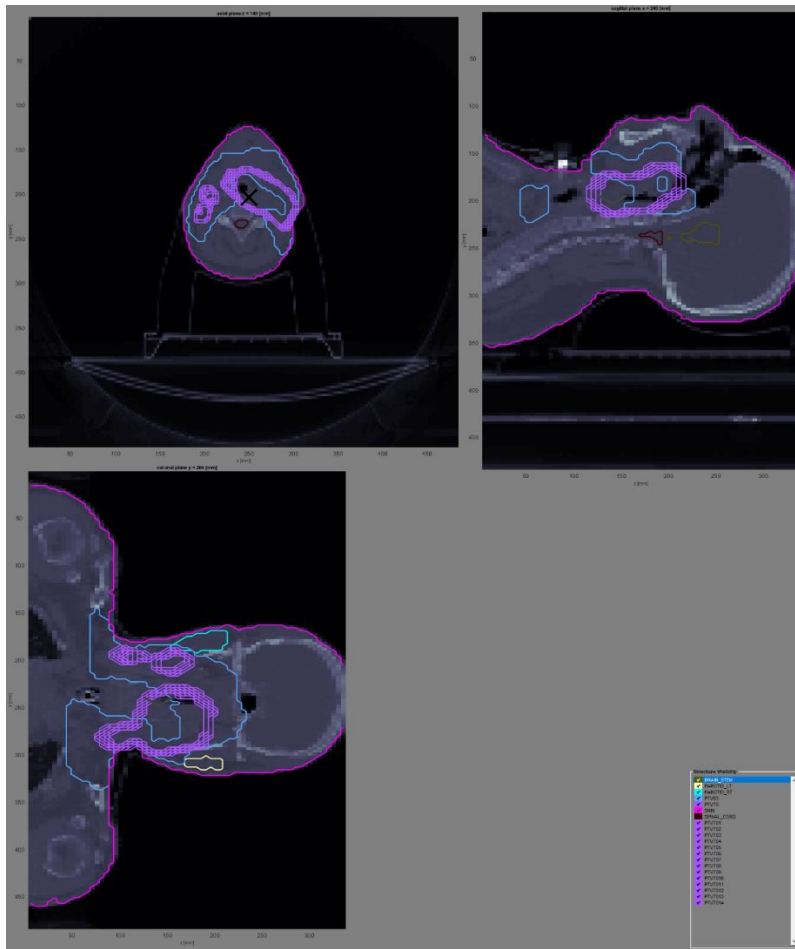
Figure 14 - *Axial, sagittal and coronal images of the head-and-neck cancer case with 14 auxiliary structures around the PTV70*

In our robust treatment planning approach, 14 additional auxiliary structures are considered in the FMO. These structures are copies of the PTV70, but in a different position considering shifts in the x, y and z axes: one for each quadrant bisector and two for each axis for both positive and negative directions. So, all these structures have exactly the same size as the original PTV70, as shown in Figure 14. The auxiliary structures were considered in the initial treatment plan, even though they are not real, they are treated equally as the PTV70. The goal of the inclusion of these structures in the optimization loop is to provide information for possible evolution of the tumour volume throughout the treatment. This methodology might also foster dose homogeneity of the final PTV70.

Four different approaches for treatment planning are being considered. Our first approach consisted in obtaining an admissible plan based only on the planning CT. This treatment planning is not accounting for any changes that might happen to the PTV70, although the definition of the PTV has, on itself, the objective of dealing with some of the existing uncertainties.

Our second approach, referred to as *New approach*, also consisted in obtaining an admissible plan based only on the planning CT, but considering an additional set of auxiliary structures similar to the PTV70 as explained before. This will change the way in which the fluences are optimized and calculated, since it will be necessary to comply with the medical prescription in more than one volume.

To acknowledge the possible improvements of adding replanning even in the presence of a robust treatment plan, the previously mentioned method was repeated but with the added feature of doing a replanning halfway through the treatment. This plan is referred to as *Replan*.

Lastly, the same treatment plan is considered but replanning is considered as often as a change in the PTV is simulated, mimicking the *Plan of the day*.

All four approaches used the FIS algorithm to change in an automated way bounds and weights of both PTV and OARs in the FMO procedure. This automated approach aims to properly irradiate the PTV70 according to the defined constraints while attempting proper OAR sparing. At each iteration of the algorithm, for every structure, the deviation between the current solution and the constraints defined for that structure is calculated. When facing uncertainty, trying to improve the dosimetric results of a given structure can have unpredictable impacts: focusing on improving a structure that will not be exactly the same during the whole treatment time can jeopardize the capability of reaching a high-quality plan under uncertainty. Moreover, as we are not considering any changes in the OARs, it does not make sense to try to spare even more these structures, since the improvements that could be obtained could be biased: we would be calculating dose in structures that might not correspond to their true situation in a real setting. For these reasons, we have focused only on reaching clinically admissible plans, with no further improvements.

When replanning, the current PTV70 is considered (the one randomly produced in the course of the treatment) as well as the other original structures.

7.3 Plan quality assessment

Whenever there is uncertainty, it is not enough to look at the dosimetric information considering the original structures of interest defined in the planning CT. To assess the performance of the four different approaches, we use Monte Carlo simulation for the case considered, taking explicitly fractionation into account. The treatment is simulated for a number of

iterations, each one of them considering the number of fractions of the treatment. During each iteration (that corresponds to one total treatment), the PTV70 will randomly change at predetermined fractions. For the approaches that consider replanning, FMO is executed, considering the current PTV at the moment of the replanning.

All the dosimetric indicators of interest are then calculated for each iteration of the simulation: The dose received by at least 95% of the PTV70 (D_{95}), mean dose (D_{mean}) for parotids, and maximum dose (D_{max}) for spinal cord, brainstem and Skin. These dosimetric indicators are calculated considering the dose deposited in each one of the voxels of the respective structures during each one of the treatment fractions.

7.4 Computational tests

Our tests were run on an Intel Core i7-8750H 2.2GHz. matRad [52], an open-source software that has been developed within the MATLAB environment, was used for dose calculation and fluence map optimization. It mimics the use of a commercial TPS, but for academic use only (Figure 12). The main advantage of this tool is that allows, in a very straightforward way, new optimization algorithms and strategies to be tested, by including new programming code in MATLAB. MATLAB version 2018b was used. matRad also provides a library of properly anonymized cases that can be used for computational tests.

The dose matrix D_{ij}, was obtained using matRad's pencil beam dose calculation engine. As previously mentioned, instead of using the built-in matRad algorithm to address the FMO, we resorted to the FIS and this approach was embedded into matRad.

A beam angle configuration of 7 equidistant coplanar angles [0 52 103 154 205 256 307] was considered, meaning that the couch angle will always be 0. This is the most usual configuration used in the clinical practice for similar cases.

Upper and lower weight penalties were defined in the beginning of the FIS FMO algorithm. For the brainstem, the spinal cord and both PTVs, higher penalty weights were attributed $\overline{\lambda} = \underline{\lambda} = 5$, while for the remaining structures $\overline{\lambda} = \underline{\lambda} = 1$. The brainstem, spinal cord and both PTVs were attributed a priority of 5 while the rest of the structures had a priority of 1. When the auxiliary structures are used, they have the same values as the PTV70 regarding priority and initial values of bounds and weights.

Inference mechanisms were created to change upper and lower bounds, to change OAR slacks based on OAR priority (greater priority, lower slack)

and to change weights when changing bounds is not enough to comply with the constraints. The algorithm will first update the upper and lower bounds of the structures. If some objectives were not met, bounds are updated accordingly. If two iterations of the algorithm are not enough to obtain the desired solution, weights are updated. If a feasible solution is met, the procedure ends otherwise slacks are created based on structure priorities, repeating the previous process.

For treatment quality assessment, the MC simulations considered 50 iterations, each with 35 fractions. A random change in the PTV is considered every 5 fractions. To avoid having any bias in the results due to the random changes generated, all the different approaches were tested considering the same sequence of random numbers, so that exactly the same PTV70 changes were considered in all the comparisons made. This structure will be changed 6 times during the course of each iteration of the simulation.

8. Results

The main objective of this study is to test and compare different treatment planning approaches, introducing a new approach based on auxiliary structures to be used in the initial treatment planning procedure. In this section we present the results of the computational experiments made.

8.1   Plan Quality

It was possible to obtain clinically admissible treatment plans considering all 50 iterations of the MC simulation for the four different approaches tested. It was thus possible to respect both upper and lower bounds defined in Table 1, for all the structures. The dosimetric measures for each OAR are presented in Figure 15 and for the PTV70 in Figure 16. The dosimetric values of all OARs for the *Conventional* and *New approach* stay the same throughout the treatment since there is not replanning and these volumes do not change in the course of the simulated treatment (Table 2). For each and every case and for all OARs it was possible to have values below the maximum threshold defined. For every case all plans respected the PTV70 thresholds established in the medical prescription.
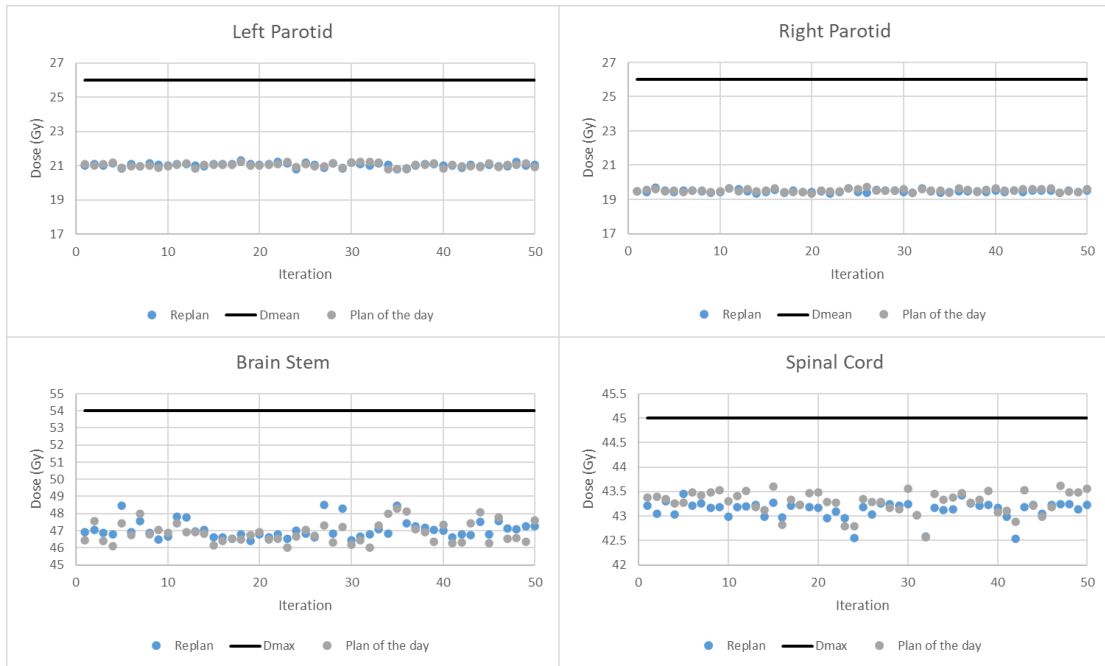
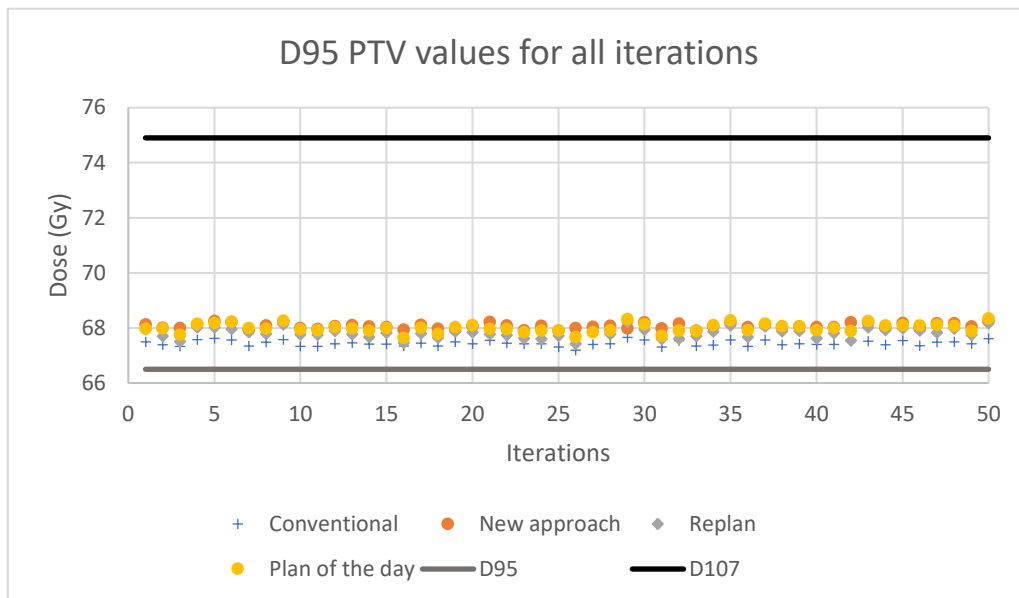**Figure 15**- *Dosimetric values for each OAR for the Replan and Plan of the day approaches*

Figure 16- *Dosimetric values for all plans regarding the PTV70*

8.2 Dosimetric comparison between approaches

The plans were evaluated regarding the obtained dosimetric values for each structure. For the PTV70, D_{95} was the considered criteria, for the brainstem and spinal cord D_{max} was considered and for the parotids D_{mean} was considered.

Table 2 displays the results obtained for the different approaches. As previously mentioned, the algorithm will not further spare the OARs, after finding proper PTV70 coverage and fulfilling the OAR threshold.

The *Conventional* approach obtained the worst result between the four plans regarding PTV70 coverage (D_{95}=67.45±0.09 Gy). On the other hand, obtained the best dosage value regarding the right parotid (D_{mean}=19.48±0.0 Gy), side by side with the *Replan* approach, since the mean values obtained are not statistically different. It also obtained one of the lowest values, statistically identical to the *Replan* and Plan of the Day approaches regarding the left parotid with D_{mean}=21.07±0.0 Gy.

The *New approach* showed the best results regarding PTV70 coverage with D_{95}=68.07 Gy, being identical to the Plan of the Day It also showed the best OAR sparing regarding the brain stem with D_{max}=44.55±0.0 Gy, alongside the Conventional approach.

The *Replan* approach behaved the best for the spinal cord, and the left parotid with mean dosimetric values of D_{max}=40.15±0.34 Gy and D_{mean}=19.48±0.08 Gy, respectively, being equivalent to the Plan of the Day. In terms of PTV70 coverage it was slightly worse (D_{95}=67.82±0.18 Gy) than the two best approaches, *Plan of the day* and *New approach*, being the means statistically different.

The *Plan of the day* showed, along with the New approach, the best PTV70 coverage results (D_{95}=68.01±0.16 Gy). It also obtained the best results regarding the left parotid sparing, with D_{mean}=21.03±0.12 Gy, and regarding the spinal cord, with D_{max}=40.20±0.45 Gy.

Table 2- Differences between the 4 plans, for the structures of interest. In green are highlighted the best results for each structure. Units are in Gray(Gy).

		Conventional		New approach		Replan		Plan of the day		Z
		Mean	SD	Mean	SD	Mean	SD	Mean	SD	
PTV70	D_{95}	67.45[a]	0.09	68.07[b]	0.09	67.82[c]	0.18	68.01[b]	0.16	204.42***
Brain Stem	D_{max}	44.71[a]	0.0	44.55[a]	0.0	45.01[b]	0.46	45.26[b]	0.49	43.86***
Spinal Cord		40.70[a]	0.0	41.01[b]	0.0	40.15[c]	0.34	40.20[c]	0.45	107.14***
Left Parotid	D_{mean}	21.07[a]	0.0	22.57[b]	0.0	21.05[a]	0.11	21.03[a]	0.12	4356.84***
Right Parotid		19.48[a]	0.0	20.08[b]	0.0	19.48[a]	0.08	19.53[c]	0.09	1303.01***

Note: Means with different letters are significantly different at the level of $\alpha < .001$ according to the post-hoc test of Tukey HSD. *** $p < .001$

Regarding PTV70 coverage, both the *New approach* and the *Plan of the day*, obtained better coverage when comparing with the *Conventional* approach for every iteration of the simulation. The *Replan* approach obtained better results in 49 out of 50 iterations, as shown in Figure 17.

When using Monte Carlo simulation, it is important to confirm that the number of iterations considered is adequate. This can be done by looking at the evolution of variation of some statistic measures, like the mean and the standard deviation. It was possible to confirm that 50 iterations were indeed sufficient. Figure 18 depicts the evolution of the mean values obtained for the dosimetric values in the OARS, as an example.
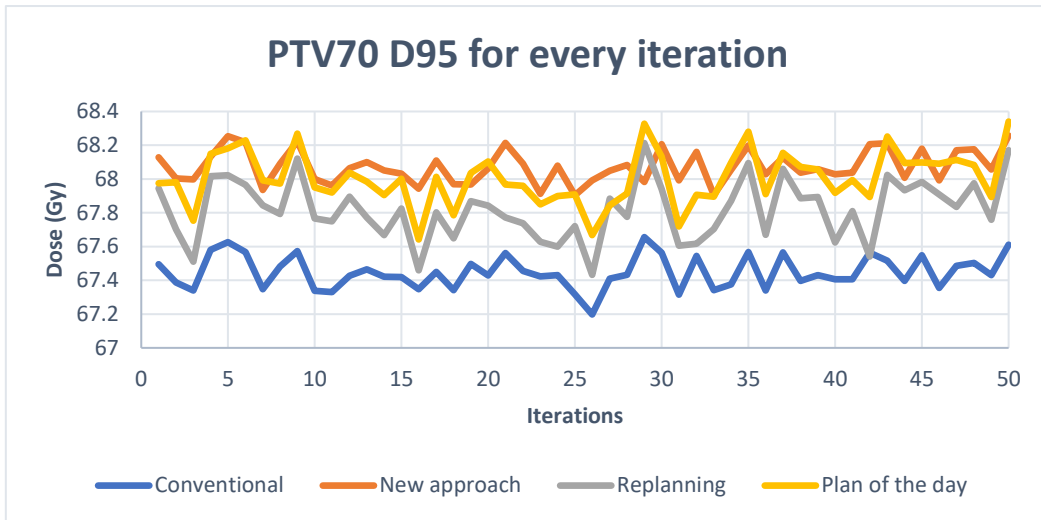
Figure 17-It is possible to see the dose difference between the plans for each of the 50 cases. Both the new approach and the plan of the day behaved similarly for some cases, giving the best result when compared with the other approaches.
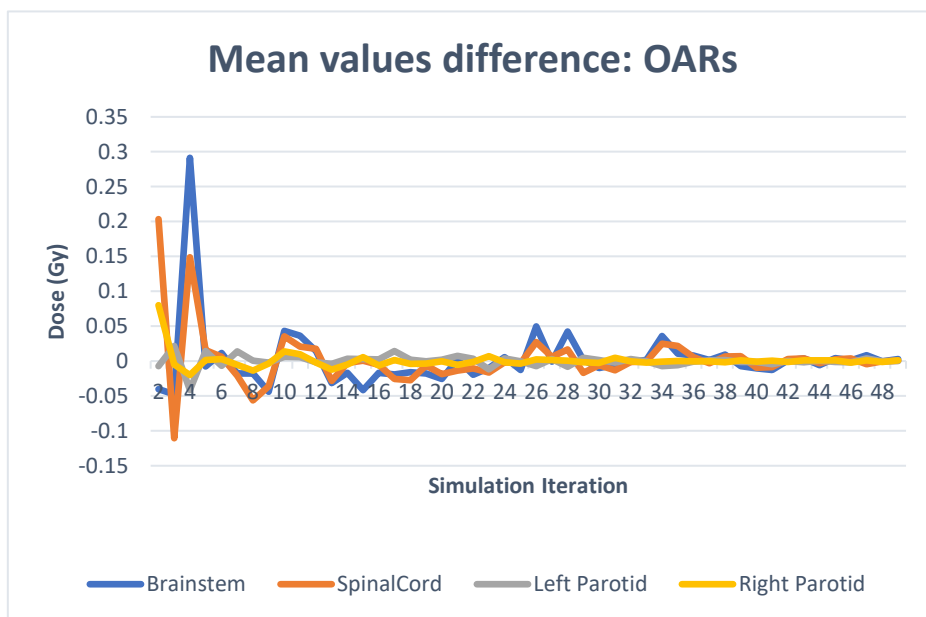

Figure 18- Evolution of the difference in the mean of OARs dosimetric measures throughout the simulation

9. Discussion and conclusion

Adaptative approaches have the advantage of using updated patient information, namely considering the delineation of all the structures of interest, during the course of the treatment to improve treatment quality. Replanning is a very important procedure in radiotherapy, usually resulting in better dosimetric results when compared to the use of a single treatment plan calculated before the beginning of the treatment.

In this work, a new approach is proposed where new auxiliary structures were created and used in the treatment planning procedure. These auxiliary structures enable a robust treatment plan to be calculated.

Four treatment planning approaches were compared, by evaluating how each one of them behaves regarding the target volume coverage while fulfilling the thresholds of the surrounding organs. All approaches were based on an automated FMO algorithm based on a FIS. MC simulation was used to compare the different approaches, considering 50 iterations, each with 35 fractions, during which the PTV was iteratively changed. It was possible to conclude that generating new auxiliary structures around the targeted area revealed enhanced PTV70 coverage when compared to Conventional plans. The PTV70 dosimetric mean results are not statistically different from the Plan of the Day. The approach also got improved brainstem sparing.

Overall, the replanning approaches showed better results in sparing the OARs, while improving the PTV70 coverage, which would be expected since they can take advantage of the knowledge regarding the decrease in the PTV volume. On the other hand, the *New approach* showed the best results improving PTV70 coverage, not statistically different from the Plan of the Day, but generally did not show better results at sparing the OARs. Moreover, the new approach presents lower standard deviation values for PTV70 than the replanning approaches. The *New approach* and the replanning approaches showed improved target coverage compared to the Conventional approach which was the main feature in study. The results proved to be consistent with the existing literature and experiments.

Although we believe the results and conclusions reached are interesting and valuable, it is also important to identify the limitations of this study.

It is important to mention that only changes to the PTV70 were considered, whilst all the other structures were considered unaltered during the course of treatment. In a real situation, all the structures suffer changes, some of which can even be correlated. Head-and-neck tumour cases have many OARs nearby the PTV and, during the treatment, when

the PTV diminishes, the tissue around it also moves, moving the surrounding OARs nearer to the target area. These changes were not replicated in the Monte Carlo simulations performed. Real head-and-neck cases also have more OARs that are usually taken into account, depending on the PTV and location, like the larynx, eyes, oral cavity, other salivary glands, etc. We have only considered 4 OARs. We have also decided to use a fixed coplanar beam configuration. Using BAO to obtain an optimized set of angles could change the obtained results, particularly when considering the possibility of using noncoplanar beam angles.

Moreover, only one case was considered, as a proof-of-concept for the new approach proposed. It would be important to repeat these computational tests with a representative set of cases to see if these results are generalisable or not.

In summary, using auxiliary structures to create a robust initial treatment plan proved to be a valid approach regarding PTV coverage. Replanning more often also showed improved PTV coverage in all cases compared to the conventional methodology while maintaining OAR sparing specially regarding the left parotid and the spinal cord. The new methodology using auxiliary structures proved to be a competitive alternative to replanning, avoiding the time-consuming replanning, and sparing the patient to further imaging sessions and all the possible disadvantages associated with this process.

As future work it would be interesting to assess the proposed approach performance for other cancer cases. Pushing beyond admissibility by using the full capacities of the FIS approach would be an important subject as well, that could change the results especially regarding OARs.

10. References

[1]   Globocan 2020, "Cancer facts 2020," 2020.
        https://gco.iarc.fr/today/data/factsheets/cancers/39-All-cancers-fact-sheet.pdf
        (accessed Dec. 10, 2021).

[2]   NORDCAN and IARC, "5-year age standardised relative survival," Sep. 27,
        2021.
        https://nordcan.iarc.fr/en/dataviz/survival?cancers=980&set_scale=0&sexes=
        1_2 (accessed Dec. 10, 2021).

[3]   "Brachytherapy to treat cancer." https://www.cancer.gov/about-
        cancer/treatment/types/radiation-therapy/brachytherapy (accessed Jan. 17,
        2022).

[4]   J. Dias, H. Rocha, B. Ferreira, and M. do C. Lopes, "A genetic algorithm with
        neural network fitness function evaluation for IMRT beam angle
        optimization," *Central European Journal of Operations Research*, vol. 22, no.
        3, pp. 431–455, 2014, doi: 10.1007/s10100-013-0289-4.

[5]   R. P. Johnson, "Review of medical radiography and tomography with proton
        beams," *Reports on Progress in Physics*, vol. 81, no. 1., Institute of Physics
        Publishing, Jan. 01, 2018. doi: 10.1088/1361-6633/aa8b1d.

[6]   Brahme A, "Solution of an integral equation encountered in rotation
        therapy," 1982. Available: http://iopscience.iop.org/0031-9155/27/10/002

[7]   G. A. Ezzell *et al.*, "Guidance document on delivery, treatment planning, and
        clinical implementation of IMRT: Report of the IMRT subcommittee of the
        AAPM radiation therapy committee," *Medical Physics*, vol. 30, no. 8, pp.
        2089–2115, Aug. 2003, doi: 10.1118/1.1591194.

[8]   J. M. Galvin, X. Chen, and R. M. Smith, "Combining multileaf fields to
        modulate fluence." *International Journal of Radiation
        Oncology*Biology*Physics* vol. 27, no. 3, pp. 697-705 (1993) doi:
        https://doi.org/10.1016/0360-3016(93)90399-G

[9]   J. H. Kung and G. T. Y. Chen, "Intensity modulated radiotherapy dose
        delivery error from radiation field offset inaccuracy," *Medical Physics*, vol.
        27, no. 7, pp. 1617–1622, 2000, doi: 10.1118/1.599028.

[10]   T. Bortfeld, "IMRT: A review and preview," *Physics in Medicine and Biology*,
        vol. 51, no. 13, pp. R363-R379, Jul. 07, 2006. doi: 10.1088/0031-
        9155/51/13/R21.

[11]   L. J. Verhey, "Comparison of Three-Dimensional Conformal Radiation
        Therapy and Intensity-Modulated Radiation Therapy Systems," *Seminars in
        Radiation Oncology,* vol. 7, no. 1, pp. 78-98 (1999). doi:
        https://doi.org/10.1016/S1053-4296(99)80056-3

[12]   P. Xia, K. K. Fu, G. W. Wong, C. Akazawa, and L. J. Verhey, "Comparison of
        treatment plans involving intensity-modulated radiotherapy for

nasopharyngeal carcinoma" *Internation Journal of Radiation Oncology*Biology*Physics* vol. 48, no. 2, pp. 329-337 (2000). doi: 10.1016/S0360-3016(00)00585-X

[13]   A. Pirzkall, M. Carol, F. Lohr, M. Wannenmacher, and U. Debus, "Comparison of intensity-modulated radiotherapy with conventional conformal radiotherapy for complex-shaped tumors." *International Journal of Radiation Oncology*Biology*Physics* vol. 48, no. 5, pp. 1371-1380 (2000) doi: 10.1016/s0360-3016(00)00772-0.

[14]   W. G. Iii and R. B. Cain, "Intensity modulated conformal therapy for intracranial lesions" *Medical Dosimetry,* vol. 23, no.3, pp. 237- 241 (1998). doi: 10.1016/S0958-3947(98)00015-6

[15]   L. Fenkell, I. Kaminsky, S. Breen, S. Huang, M. van Prooijen, and J. Ringash, "Dosimetric comparison of IMRT vs. 3D conformal radiotherapy in the treatment of cancer of the cervical esophagus," *Radiotherapy and Oncology*, vol. 89, no. 3, pp. 287–291, Dec. 2008, doi: 10.1016/j.radonc.2008.08.008.

[16]   K. Otto, "Volumetric modulated arc therapy: IMRT in a single gantry arc," *Medical Physics*, vol. 35, no. 1, pp. 310–317 (2008), doi: 10.1118/1.2818738.

[17]   H. Rocha and J. M. Dias, "On the Optimization of Radiation Therapy Planning," 2009, [Online]. Available: www.inescc.pt

[18]   P. Carrasqueira, H. Rocha, J. M. Dias, T. Ventura, B. C. Ferreira, and M. C. Lopes, "An automated treatment planning strategy for highly noncoplanar radiotherapy arc trajectories" 2021. doi: doi.org/10.1111/itor.12953 PMID: 9711744

[19]   M. Bangert, P. Ziegenhein, and U. Oelfke, "Comparison of beam angle selection strategies for intracranial IMRT," *Medical Physics*, vol. 40, no. 1, pp. 011716 (2013), doi: 10.1118/1.4771932.

[20]   R. Adler Jr. J, D. Chang S, J. Murphy M, Doty J, Geis P, and L. Hancock S, "The Cyberknife: A Frameless Robotic System for Radiosurgery," *Stereotact Funct Neurosurg*, 69(1-4 Pt 2):124-8 1997, doi: 10.1159/000099863.

[21]   H. Rocha, J. M. Dias, B. C. Ferreira, and M. C. Lopes, "Otimização do planeamento inverso de tratamentos em radioterapia," 2013.

[22]   B. Fraass *et al.*, "American association of physicists in medicine radiation therapy committee task group 53: Quality assurance for clinical radiotherapy treatment planning," *Medical Physics*, vol. 25, no. 10, pp. 1773–1829, 1998, doi: 10.1118/1.598373.

[23]   S. Ahmed, O. Gozbasi, M. Savelsbergh, I. Crocker, T. Fox, and E. Schreibmann, "A Fully-Automated Intensity-Modulated Radiation Therapy Planning System." Available: www. isye.gatech.edu/sahmed/imrt-final.pdf.

[24]   S. Breedveld, P. R. M. Storchi, P. W. J. Voet, and B. J. M. Heijmen, "ICycle: Integrated, multicriterial beam angle, and profile optimization for generation

of coplanar and noncoplanar IMRT plans," *Medical Physics*, vol. 39, no. 2, pp. 951–963, 2012, doi: 10.1118/1.3676689.

[25] H. Rocha, J. Dias, T. Ventura, B. Ferreira, and M. D. C. Lopes, "A derivative-free multistart framework for an automated noncoplanar beam angle optimization in IMRT," *Medical Physics*, vol. 43, no. 10, pp. 5514–5526, Oct. 2016, doi: 10.1118/1.4962477.

[26] M. Ehrgott, Ç. Güler, H. W. Hamacher, and L. Shao, "Mathematical optimization in intensity modulated radiation therapy," *4OR*, vol. 6, no. 3, pp. 199–262 (2008), doi: 10.1007/s10288-008-0083-7.

[27] H. Rocha, J. M. Dias, B. C. Ferreira, and M. C. Lopes, "Combinatorial optimization for an improved transition from fluence optimization to fluence delivery in IMRT treatment planning," *Optimization*, vol. 61, no. 8, pp. 969–987, Aug. 2012, doi: 10.1080/02331934.2011.607498.

[28] D. M. Shepard, M. A. Earl, X. A. Li, S. Naqvi, and C. Yu, "Direct aperture optimization: A turnkey solution for step-and-shoot IMRT," *Medical Physics*, vol. 29, no. 6, pp. 1007–1018, (2002), doi: 10.1118/1.1477415.

[29] G. Bednarz *et al.*, "The use of mixed-integer programming for inverse treatment planning with pre-defined field segments" *Institute of physics publishing physics in medicine* 2002. [Online]. Available: http://iopscience.iop.org/0031-9155/47/13/304

[30] C. Men, H. E. Romeijn, Z. C. Taşkin, and J. F. Dempsey, "An exact approach to direct aperture optimization in IMRT treatment planning," *Physics in Medicine and Biology*, vol. 52, no. 24, pp. 7333–7352, Dec. 2007, doi: 10.1088/0031-9155/52/24/009.

[31] M. Alber and F. Nüsslin, "Optimization of intensity modulated radiotherapy under constraints for static and dynamic MLC delivery" *Institute of physics publishing physics in medicine* 2001. [Online]. Available: http://iopscience.iop.org/0031-9155/46/12/311

[32] X. Li *et al.*, "Automatic IMRT planning via static field fluence prediction (AIP-SFFP): a deep learning algorithm for real-time prostate treatment planning," *Physics in Medicine & Biology*, vol. 65, no. 17, p. 175014, Sep. 2020, doi: 10.1088/1361-6560/aba5eb.

[33] M. Zarepisheh *et al.*, "A DVH-guided IMRT optimization algorithm for automatic treatment planning and adaptive radiotherapy replanning," *Medical Physics*, vol. 41, no. 6, pp. 061711 (2014), doi: 10.1118/1.4875700.

[34] Q. Jia *et al.*, "OAR dose distribution prediction and gEUD based automatic treatment planning optimization for intensity modulated radiotherapy," *IEEE Access*, vol. 7, pp. 141426–141437, 2019, doi: 10.1109/ACCESS.2019.2942393.

[35] B. W. K. Schipaanboord, M. K. Giżyńska, L. Rossi, K. C. de Vries, B. J. M. Heijmen, and S. Breedveld, "Fully automated treatment planning for MLC-

based robotic radiotherapy," *Medical Physics*, vol. 48, no. 8, pp. 4139–4147, Aug. 2021, doi: 10.1002/mp.14993.

[36] R. Bijman *et al.*, "First system for fully-automated multi-criterial treatment planning for a high-magnetic field MR-Linac applied to rectal cancer," *Acta Oncologica*, vol. 59, no. 8, pp. 926–932, Aug. 2020, doi: 10.1080/0284186X.2020.1766697.

[37] G. Wortel *et al.*, "Characterization of automatic treatment planning approaches in radiotherapy," *Physics and Imaging in Radiation Oncology*, vol. 19, pp. 60–65, Jul. 2021, doi: 10.1016/j.phro.2021.07.003.

[38] S. Cilla *et al.*, "Personalized Treatment Planning Automation in Prostate Cancer Radiation Oncology: A Comprehensive Dosimetric Study," *Frontiers in Oncology*, vol. 11, Jun. 2021, doi: 10.3389/fonc.2021.636529.

[39] J. Dias, H. Rocha, T. Ventura, B. Ferreira, and M. D. C. Lopes, "Automated fluence map optimization based on fuzzy inference systems," *Medical Physics*, vol. 43, no. 3, pp. 1083–1095, Mar. 2016, doi: 10.1118/1.4941007.

[40] Y. Elcim, B. Dirican, and O. Yavas, "Dosimetric comparison of pencil beam and Monte Carlo algorithms in conformal lung radiotherapy," *Journal of Applied Clinical Medical Physics*, vol. 19, no. 5, pp. 616–624, Sep. 2018, doi: 10.1002/acm2.12426.

[41] T. Krieger and O. A. Sauer, "Monte Carlo- versus pencil-beam-/collapsed-cone-dose calculation in a heterogeneous multi-layer phantom," in *Physics in Medicine and Biology*, vol. 50, no. 5, pp. 859–868, Mar. 2005. doi: 10.1088/0031-9155/50/5/010.

[42] T. S. Hong, W. A. Tomé, R. J. Chappell, P. Chinnaiyan, M. P. Mehta, and P. M. Harari, "The impact of daily setup variations on head-and-neck intensity-modulated radiation therapy," *International Journal of Radiation Oncology Biology Physics*, vol. 61, no. 3, pp. 779–788, (2005), doi: 10.1016/j.ijrobp.2004.07.696.

[43] A. Dutreix, "When and how can we improve precision in radiotherapy?," *Radiother Oncol.,* vol. 2, no. 4, pp. 275-292 (1984). doi: 10.1016/s0167-8140(84)80070-5

[44] L. Verhey, "Immobilizing and Positioning Patients for Radiotherapy." *Seminars in Radiation Oncology* vol.5, no. 2, pp. 100-114, Apr. 1995 doi: 10.1016/S1053-4296(95)80004-2

[45] D. Yan and J. Liang, "Expected treatment dose construction and adaptive inverse planning optimization: Implementation for offline head and neck cancer adaptive radiotherapy," *Medical Physics*, vol. 40, no. 2, 2013, doi: 10.1118/1.4788659.

[46] J. L. Barker *et al.*, "Quantification of volumetric and geometric changes occurring during fractionated radiotherapy for head-and-neck cancer using an integrated CT/linear accelerator system," *International Journal of*

Radiation Oncology Biology Physics, vol. 59, no. 4, pp. 960–970, Jul. 2004, doi: 10.1016/j.ijrobp.2003.12.024.

[47]   E. K. Hansen, M. K. Bucci, J. M. Quivey, V. Weinberg, and P. Xia, "Repeat CT imaging and replanning during the course of IMRT for head-and-neck cancer," *International Journal of Radiation Oncology Biology Physics*, vol. 64, no. 2, pp. 355–362, Feb. 2006, doi: 10.1016/j.ijrobp.2005.07.957.

[48]   E. M. Vásquez Osorio, M. S. Hoogeman, A. Al-Mamgani, D. N. Teguh, P. C. Levendag, and B. J. M. Heijmen, "Local Anatomic Changes in Parotid and Submandibular Glands During Radiotherapy for Oropharynx Cancer and Correlation With Dose, Studied in Detail With Nonrigid Registration," *International Journal of Radiation Oncology Biology Physics*, vol. 70, no. 3, pp. 875–882, Mar. 2008, doi: 10.1016/j.ijrobp.2007.10.063.

[49]   S. van Kranen, A. Mencarelli, S. van Beek, C. Rasch, M. van Herk, and J. J. Sonke, "Adaptive radiotherapy with an average anatomy model: Evaluation and quantification of residual deformations in head and neck cancer patients," *Radiotherapy and Oncology*, vol. 109, no. 3, pp. 463–468, Dec. 2013, doi: 10.1016/j.radonc.2013.08.007.

[50]   J. J. Sonke, M. Aznar, and C. Rasch, "Adaptive Radiotherapy for Anatomical Changes," *Seminars in Radiation Oncology*, vol. 29, no. 3. W.B. Saunders, pp. 245–257, Jul. 01, 2019. doi: 10.1016/j.semradonc.2019.02.007.

[51]   V. Murthy *et al.*, "'Plan of the day' adaptive radiotherapy for bladder cancer using helical tomotherapy," *Radiotherapy and Oncology*, vol. 99, no. 1, pp. 55–60, Apr. 2011, doi: 10.1016/j.radonc.2011.01.027.

[52]   Wieser, Hans-Peter, et al. "Development of the open-source dose calculation and optimization toolkit matRad." Medical physics 44.6 (2017): 2556-2568.